ADVANCED THERAPEUTICS
www.advtherap.com

Surfactant-Stripped Cabazitaxel Micelles Stabilized by Clotrimazole or Mifepristone

*Boyang Sun, Upendra Chitgupi, Changning Li, Jasmin Federizon, Changjie Zhang, Donna M. Ruszaj, Aida Razi, Joaquin Ortega, Sriram Neelamegham, Yumiao Zhang, and Jonathan F Lovell**

Taxane chemotherapy formulations are used to treat advanced cancers, but limited solubility and propensity for aggregation in water complicates their development. Many involve drug dissolution in organic solvents and liquid surfactants, or use of lyophilization and reconstitution approaches. "Surfactant-stripping," has been previously reported, in which hydrophobic drugs were first dispersed in Pluronic (Poloxamer) surfactant, then subjected to membrane processing below the critical micelle temperature, to remove free and loose surfactant while retaining the active cargo. In the present work, stabilized, surfactant-stripped (sss) cabazitaxel (CTX) micelles with potential for long-term aqueous storage are developed. Some 50 hydrophobic co-loaders cargos are screened for capacity to prevent aggregation of CTX, of which approximately 10 are effective. Further screening identifies the antifungal clotrimazole and the abortificant mifepristone as the most effective stabilizers for sss-CTX micelles, via interference with the CTX aggregation process. Micelles remain stable for hundreds of days in aqueous storage and suppress the growth of orthotopic 4T1 murine mammary tumors. Pharmacokinetics, tubulin stabilization, and neutropenia induction of sss-CTX are generally comparable to a TWEEN-80 CTX formulation. These data reveal sss-CTX as a taxane delivery vehicle with a high drug-to-surfactant ratio and capacity for extended aqueous storage.

1. Introduction

Taxanes, including paclitaxel (PTX), docetaxel (DTX), and cabazitaxel (CTX) are microtubule stabilizing agents with broad spectrum anti-tumor activity, and are used for treating ovarian, lung, breast, and prostate cancers, amongst others.[1] The first taxane, PTX, has been developed into numerous clinically-tested formulations, however drug resistance, which is often attributed to increased P-glycoprotein expression, is an inherent problem that is difficult to overcome.[2] Aiming to overcome resistance, analogs of PTX have been screened and tested.[3] CTX is a second generation taxane, designed to have low affinity to P-glycoprotein and activity in cancer cells resistant to DTX.[3] In a phase III trial in metastatic prostate cancer patients, CTX and prednisone induced longer overall survival (15.1 months) compared to mitoxantrone and prednisone (12.7 months).[4] CTX was approved for metastatic castration-resistant prostate cancer by the United States Food and Drug Administration in 2010.[5]

Since CTX is not soluble in water, exogenous excipients such as surfactants or ethanol can be used for dissolving the drug prior to intravenous administration. The current clinical CTX formulation (trade name Jevtana), is a polysorbate (TWEEN) formulation. Every 40 mg of cabazitaxel is dissolved in 1 mL of liquid TWEEN-80 and the drug is diluted in a 13% ethanol solution as an intermediate preparation step prior to administration. In recent years, many novel preclinical CTX formulations have emerged in research studies.[6] These include formulations based on serum albumin,[7–10] liposomes,[11,12] lipid nanoparticles,[13,14] polymeric micelles,[15,16] polymer nanoparticles,[17,18] and covalent conjugates.[19–21]

B. Sun, Dr. U. Chitgupi, Dr. J. Federizon, Prof. J. F Lovell
Department of Biomedical Engineering, University at Buffalo
State University of New York (SUNY)
Buffalo, NY 14260, USA
E-mail: jflovell@buffalo.edu

B. Sun, C. Li, C. Zhang, Prof. S. Neelamegham, Prof. J. F Lovell
Department of Chemical and Biological Engineering, University at Buffalo
SUNY
Buffalo, NY 14260, USA

D. M. Ruszaj
Department of Pharmaceutical Sciences
University at Buffalo
SUNY
Buffalo, NY 14260, USA

A. Razi, Prof. J. Ortega
Department of Anatomy and Cell Biology
Mcgill University
Montreal, Quebec L8S4L8, Canada

Prof. Y. Zhang
School of Chemical Engineering and Technology
Tianjin University
Tianjin 301636, China

The ORCID identification number(s) for the author(s) of this article can be found under https://doi.org/10.1002/adtp.201900161

DOI: 10.1002/adtp.201900161

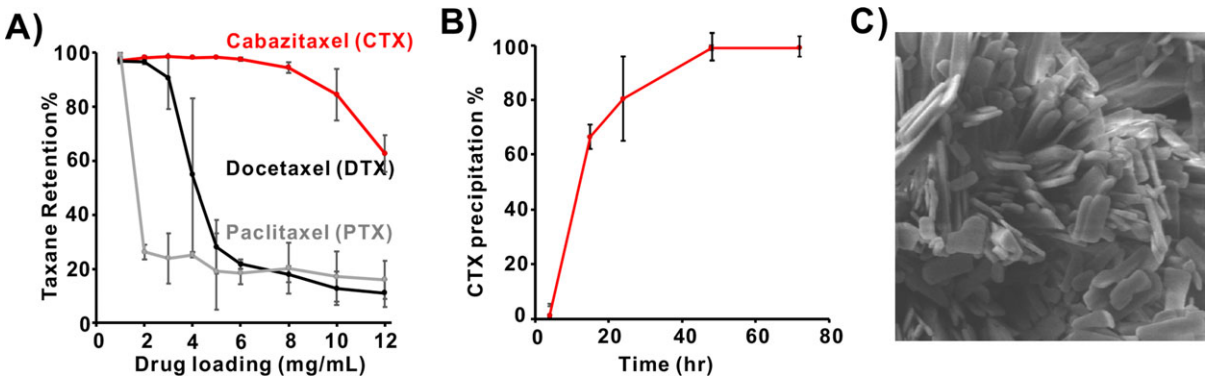

Figure 1. Taxane aggregation in F127 micelles. A) Taxane retention in Pluronic F127 micelles (10% w/v F127) in the supernatant following drug dissolution and centrifugation. B) Aggregation kinetics of CTX dissolved after 15-fold dilution in PBS. Values show mean ± SD for $n = 3$. C) Scanning electron micrograph of CTX that aggregated in F127 solution. Full image width corresponds to 6.5 µm.

The aqueous stability of taxane drug formulations is a concern, due to propensity for aggregation. Formulations that are directly prepared in pure surfactants solutions can be viscous, induce foaming and plasticizer leaching,[22] and in vivo excess surfactant can modulate pharmacokinetics[23] and induce hypersensitivity infusion reactions.[24] Alternate approaches such as Abraxane (a commercial albumin-based PTX formulation) and Genexol-PM (polymeric micelle PTX formulation) use a lyophilized powder, which has an extended shelf life to address storage stability issues. However, the reconstitution protocol can give rise to foaming and calls for immediate drug administration, as aggregation occurs relatively rapidly after reconstitution. This is unlike other nanomedicines like Doxil, a liposomal suspension of doxorubicin which is prepared and stored as liquid. A stable aqueous formulation could have advantages for simpler preparation for administration.

We reported a drug delivery approach based on surfactant-stripped micelles, in which Pluronic F127 (also known as Poloxamer 407), which has a temperature sensitive micellization temperature, is first used to dissolve hydrophobic drugs; then, the temperature is lowered to convert loose and free surfactant into unimers, which can be removed by membrane filtration.[25] This approach was previously applied to CTX, however, in that case highly hypertonic saline was required, as was the use of a hydrophobic "co-loader," Coenzyme Q10, which was found to inhibit taxane aggregation. Hypertonic saline complicates surfactant-stripping since salt also decreases the critical micelle temperature, necessitating membrane processing at sub-zero temperatures.[26] Furthermore, aggregation became apparent in surfactant-stripped CTX micelles with storage after a few days. We hypothesized that identification of an improved "co-loader" could lead to stabilized surfactant-stripped micelles (sss-micelles) with extended aqueous storage stability while maintaining therapeutic efficacy.

2. Results

2.1. Taxane Aggregation in Pluronic F127 Micelles

Three members of the taxane family (PTX; DTX; CTX) were assessed for solubility in Pluronic F127 (F127) micelles. The organic solvent dichloromethane (DCM) was used to first dissolve the taxanes, which were then added dropwise to a stirring 10% F127 (w/v) solution that was stirred until the DCM evaporated. Solubility was then assessed as drug retention in the supernatant following centrifugation. As **Figure 1**A shows, CTX had higher solubility in F127, up to 6 mg mL^{-1}, compared to DTX and PTX (1 mg mL^{-1} and 2 mg mL^{-1}, respectively). This may stem from the somewhat higher lipophilicity of CTX compared to other taxanes (CTX has a log *P* partition coefficient of 3.7, whereas DTX has a log *P* of 2.6, and PTX has a log P of 3.2).[27]

The stability of CTX in dissolved aqueous F127 micelles was next examined. Although CTX could be dissolved in 10% F127 at 6 mg mL^{-1}, a lower dose of 4 mg mL^{-1} was used to ensure complete dissolution. The clear solution was diluted 15-fold in phosphate buffered saline (PBS), so that the F127 concentration was lower than its critical micelle concentration (CMC), thereby diminishing the micelle population.[28] In these dilute conditions, CTX aggregated within 2 days (Figure 1B). Scanning electron microscopy (SEM) of the precipitates revealed an ordered and crystal-like morphology (Figure 1C).

2.2. Co-Loaders can Inhibit CTX Aggregation in F127 Micelles

To determine whether other hydrophobic cargo co-localized within the F127 micelles could increase CTX aqueous storage stability, we developed an assay to screen over 50 compounds, mostly approved drugs and vitamins, for inhibiting CTX aggregation. Co-loader cargos were mixed with CTX at a 20% mass ratio and co-dissolved in a stirring F127 solution. Following organic solvent evaporation, the resulting mixture was then diluted 15-fold, to below the F127 CMC, and 2 days later the amount of non-aggregated drug was quantified. As shown in **Figure 2**A, while the majority of hydrophobic cargo did not inhibit CTX precipitation, several did so. Co-loaders such as selamectin, mifepristone (MIF), clotrimazole (CLT), ketoconazole, and ivermectin significantly inhibited CTX aggregation during the 2-day storage period. Examination of some drug families showed patterns of compounds that prevented CTX aggregation, such as the ivermectin family of anthelmintics used to treat parasites and insect pests (Figure 2B). Ivermectin, doramectin, selamectin, abamectin all were effective in preventing CTX

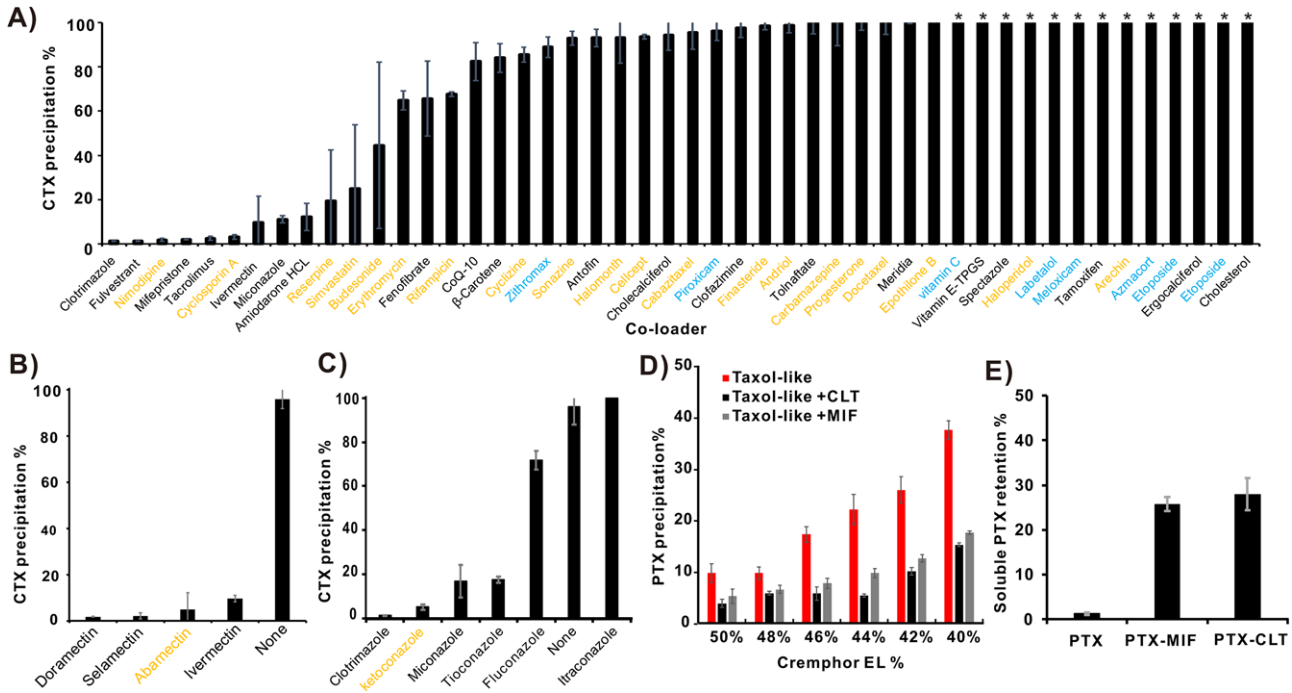

Figure 2. Identification of co-loaders which prevent taxane aggregation. A) Screening hydrophobic co-loaders for inhibition of aggregation of F127-dispersed CTX. CTX and co-loaders were dispersed in F127, diluted, and stored at room temperature for 2 days prior to assessing precipitation. Asterisks denote co-loaders which could not form F127 micelles with CTX. Co-loaders with log $P > 5$ are written in black, those with log P between 2.5 and 5 are written in yellow, and those with log $P < 2.5$ are written in blue. B) Screening ivermectin drug family members for inhibiting CTX aggregation in F127 micelles. C) Screening antifungal co-loaders for CTX aggregation inhibition. D) CLT and MIF prevention of aggregation following dilution of a Taxol-like formulation (i.e., PTX formulated in Cremophor EL:ethanol, 1:1 volume ratio) to the indicated Cremophor EL concentrations. E) CLT or MIF induced inhibition of PTX aggregation of an albumin-based PTX formulation. Values show mean ± SD for $n = 3$ measurements.

aggregation in F127 micelles in a 2-day storage period. Another class of drugs that was effective in preventing CTX aggregations was the antifungal agents CLT, ketoconazole, miconazole, tioconazole, and fluconazole (Figure 2C). The log P of the co-loaders, which is shown in color coding in Figure 2, did not correlate with which co-loaders were effective at CTX stabilization, nor did other co-loader molecular properties examined (such as polarizability, physiological charge, number of rings, hydrogen acceptor count, and refractivity) as shown by poor correlation between CTX stabilization and these parameters (Figure S1, Supporting Information).

We next sought to determine whether co-loaders could have broader stabilizing utility, beyond CTX and low-surfactant F127 micelles. Taxol is an ethanol and Cremphor EL based PTX formulation and Abraxane is an albumin-bound PTX formulation.[29,30] CLT and MIF, two promising co-loaders identified in the screen, were assessed for inhibiting PTX aggregation in surfactant- and albumin- based formulations. As shown in Figure 2D, both CLT and MIF, when incorporated at 25% of the mass of PTX, resulted in diminished PTX aggregation of the ethanol and Cremophor-EL PTX formulation following varying degrees dilution and storage for 2 days. An albumin-based PTX formulation was prepared, with or without the inclusion of CLT or MIF. After 2 days of storage, the PTX albumin formulation had completely aggregated, whereas CLT or MIF inclusion partially inhibited aggregation (Figure 2E). Therefore, although this study focuses on stabilized, surfactant-stripped CTX micelles (sss-micelles), the use of these co-loaders may be versatile for aqueous formulations with improved storage stability for diverse solubilizing agents and taxanes.

2.3. Cargo Co-Loading Stabilizes Surfactant-Stripped CTX

We next examined those co-loaders which inhibited at least 95% of the CTX aggregation over 2 days of storage, of which ten were identified from the preliminary screen (CLT, fulvestrant, nimodipine, MIF, tacrolimus, cyclosporin A, doramectin, selamectin, abamectin, and ketoconazole). Although the initial screening had mimicked one aspect of the surfactant-stripping in the sense that the assay involved dilution of F127 to below its CMC, actual surfactant-stripping was next carried out for these 10 co-loaders. **Figure 3**A schematically illustrates the F127 stripping process, showing how low-temperature membrane processing removes free and loose surfactant. CTX retention with various co-loaders was examined after the washing process, as the drug may escape or get caught through the filter, or may aggregate during the process. Figure 3B that shows the addition of co-loaders modestly improved post-stripping CTX retention relative to surfactant-stripping without any co-loader. Drug retention was generally between 50–80%. After the stripping process, the stability of stabilized, surfactant-stripped CTX (sss-CTX) was assessed with storage at 25 or 4 °C for up to 4 weeks. As shown in Figure 3C,D, storage at 4 °C improved stability compared to room

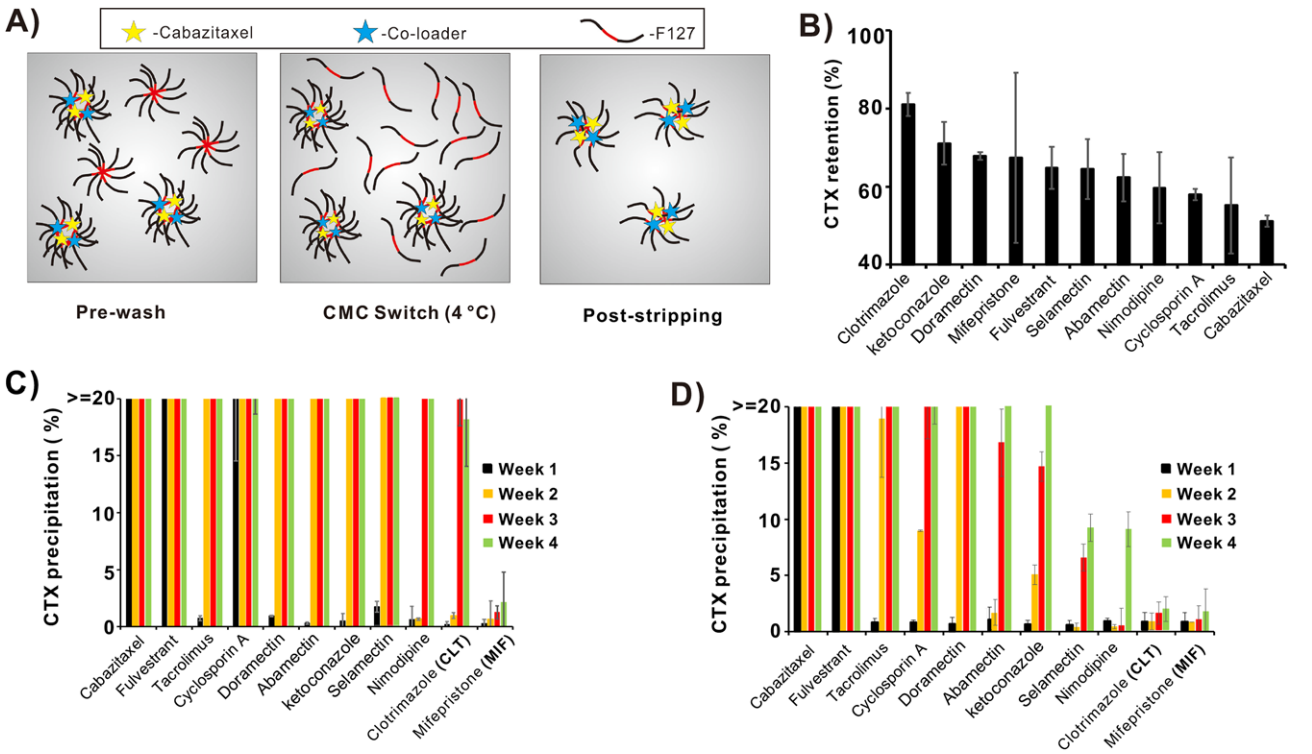

Figure 3. MIF and CLT stabilize surfactant-stripped CTX. A) Schematic illustration of the low-temperature surfactant-stripping process used with F127 surfactant. Lowering the temperature changes the CMC of F127, converting free and loose micelles into unimers. B) CTX retention during surfactant-stripping with various co-loaders. Stabilized, surfactant-stripped CTX (sss-CTX) stability during indicated storage time at room temperature C) or 4 °C D). Values show mean ± SD for $n = 3$ measurements.

temperature for most co-loaders. Without co-loading, surfactant-stripped CTX alone had aggregated by the first week, as expected. Most co-loaders induced some degree of prevention against CTX aggregation during the first week of storage, but at room temperature, only MIF resulted in 4 weeks of storage stability without more than 5% aggregation. At 4 °C, MIF, as well as CLT co-loading resulted in storage stability without aggregation. Based on these results, MIF-sss-CTX and CLT-sss-CTX were assessed for further studies.

2.4. Co-Loaders MIF and CLT Inhibit CTX Aggregation in F127 Micelles

To gain insight into the mechanism of stabilization, 2D-NMR was assessed of CTX with co-loaders. The NMR spectra with 50 mg mL^{-1} CTX and co-loaders were acquired in deuterated chloroform, which may potentially mimic the interactions encountered in the hydrophobic core of the F127 micelles (MIF: Figure S2A, Supporting Information, CLT: Figure S2B, Supporting Information). In general, the NOESY spectra did not reveal substantial intermolecular interactions between CTX and co-loader. However, one specific interaction between MIF and CTX was observable and is shown in the chemical structures in **Figure 4**A. The interacting protons are labeled with red circles in CTX and MIF. No intermolecular interactions between CLT and CTX were observed by 2D NMR (Figure S2B, Supporting Information). However, owing to strong proton overlap between CLT and CTX, the absence of such signal does not mean that there was a lack of stabilizing intermolecular interactions. We hypothesized that the co-loader might interfere with the CTX crystallization process. To assess the morphology of CTX aggregates, SEM with or without co-loaders present was assessed. Since the co-loader stabilized the micelles, some precipitation was collected after 600 days of storage of sss-CTX. As shown in Figure 4B, a crystal-like structure was observed with precipitated CTX by SEM. X-ray powder diffraction confirmed the crystalline nature of the aggregate (Figure S3, Supporting Information). The addition of MIF prevented the emergence of crystalline structures as observed by SEM and X-ray diffraction, and resulted in an amorphous CTX structure (Figure 4C; Figure S4, Supporting Information). Interestingly, CLT did not appear to clearly inhibit crystallization, and some crystal-like morphology was observed by both SEM and X-ray diffraction (Figure 4D; Figure S5, Supporting Information). The stabilization of CTX by MIF therefore is straightforward to describe, owing to specific atomic interactions between CTX and MIF, and prevention of CTX crystallization in extended storage. Nevertheless, CLT was also an effective stabilizer of CTX, despite an absence of molecular evidence for how CLT stabilizes CTX.

2.5. Scale-Up of Stabilized, Surfactant-Stripped CTX

Pilot studies made use of sss-CTX generated by low temperature microcentrifugal filtration in order to strip F127. Large-scale studies, with gram scale formulation of CTX, made use of

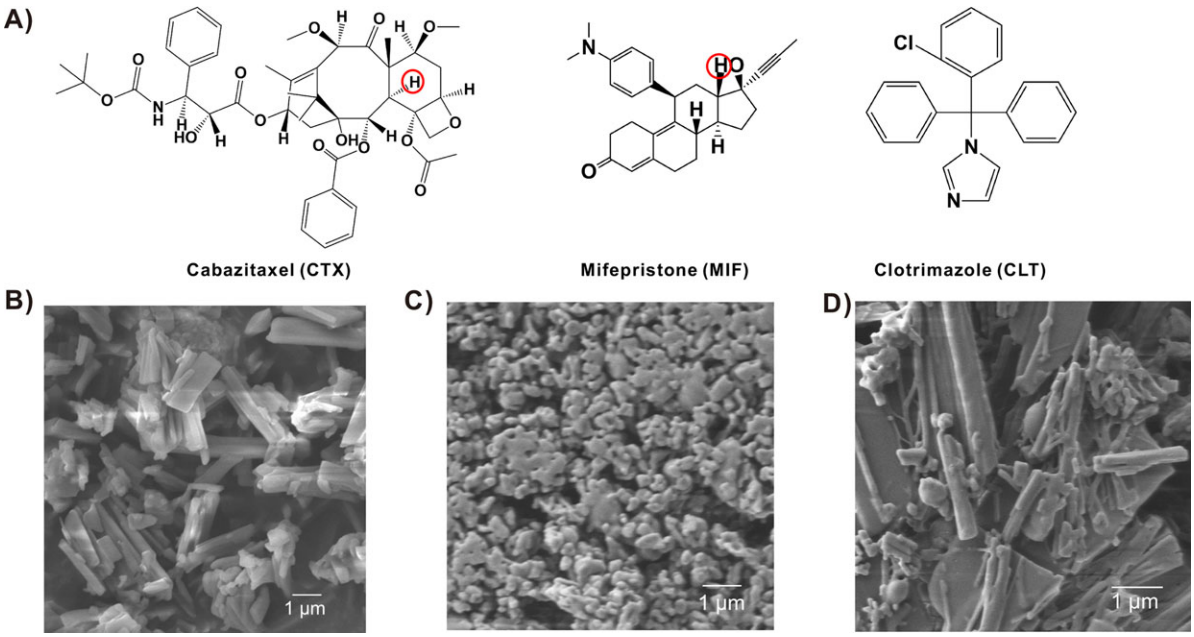

Figure 4. Co-loaders interfere with CTX aggregation. A) Chemical structure of CTX, MIF and CLT. The red circles shown on CTX and MIF indicate specific proton interaction detected by 2D NMR. SEM is shown of lyophilized, washed precipitates of surfactant-stripped CTX alone B), or stabilized MIF-sss-CTX C) or CLT-sss-CTX D). sss-CTX samples were collected from small precipitation observed following 600 days of storage at 4 °C.

a scalable diafiltration system with cooling provided by an ice bath. As shown in **Figure 5**A, during surfactant-stripping with CTX and CLT co-loaded, bulk and loose F127 was effectively removed during the process, while CLT was completely retained. Approximately 20% of the CTX was gradually lost during the stripping process, likely indicating the drug left through the filtration membrane pores. Comparable results were obtained for MIF-sss-CTX, as shown in Figure 5B. As **Table 1** shows, sss-CTX has a CTX to F127 molar ratio of 3–4, which is nearly a two order of magnitude higher drug-to-surfactant molar ratio compared to the TWEEN-80 (Jevtana) formulation.

In long-term storage, CLT-sss-CTX and MIF-sss-CTX maintained stable nanoparticle size and PDI for hundreds of days (Figure 5C,D). Also, the drug content after sterile filtration stayed stable for at least 300 days, indicating that a stable CTX formulation was achieved (Figure 5E). Cryo-electron microscopy (cryo-EM) revealed that CLT-sss-CTX (Figure 5F) and MIF-sss-CTX (Figure 5G) formed spherical particles that were homogenous in size. The slightly larger observed size of CLT-sss-CTX compared to MIF-sss-CTX was consistent with dynamic light scattering (DLS) results. The cryo-EM images showed MIF-sss-CTX to have diameter roughly of 40 nm, whereas DLS showed a diameter close to 60 nm. The outer polyethylene glycol shell of the micelles may have contributed to the hydrodynamic radius but was not visible by cryo-EM.

2.6. In Vitro Activity of sss-CTX

The main mechanism of the action of CTX is to stabilize the tubulin polymerization, leading to cellular apoptosis.[27] Microtubule polymerization was evaluated using a porcine tubulin assay. As shown in **Figure 6**A, various taxane solutions accelerated microtubulin polymerization as expected. Vinblastine, a tubulin polymerization inhibitor, served as a negative control. The co-loaders themselves did not impact tubulin polymerization. When sss-CTX was assessed at the same concentration, the formulations showed similar capacity to stabilize microtubules as a Jevtana-like TWEEN-80 formulation (Figure 6B). Further, there was no difference in microtubule stabilization pre- and post-CTX stripping. This is an interesting observation and implies that the drug in surfactant-stripped micelles is in dynamic equilibrium and able to be immediately accessible to tubulin.

Next, a hemolysis assay was carried out to determine whether the low surfactant sss-CTX is benign to red blood cells. Freshly collected human erythrocytes were incubated with various formulations at 37 °C, along with a negative control and positive control (PBS and Triton X-100). As **Figure 7**A shows, there was no hemolysis induced by sss-CTX, in contrast to the TWEEN-80 CTX formulation, which induced significant hemolysis that increased with CTX concentration. It should be noted that hemolysis is not a problem in clinical administration of Jevtana. It is also known than TWEEN-80 is not a completely inert compound, it can activate a complement cascade and induce an acute hypersensitive reaction.[31] The level of the complement activation was measured by a SC5b-9 enzyme-linked assay kit. When incubated with human plasma, the TWEEN-80 based formulation induced higher complement activation product (sc5b-9) than sss-CTX (Figure 7B).

2.7. Antitumor Activity of sss-CTX

Antitumor efficacy was evaluated in orthotopic murine 4T1 mammary tumors at three different dosing regimes: 30 mg $kg^{-1} \times 2$; 15 mg $kg^{-1} \times 3$; and 8 mg $kg^{-1} \times 3$ injections. The

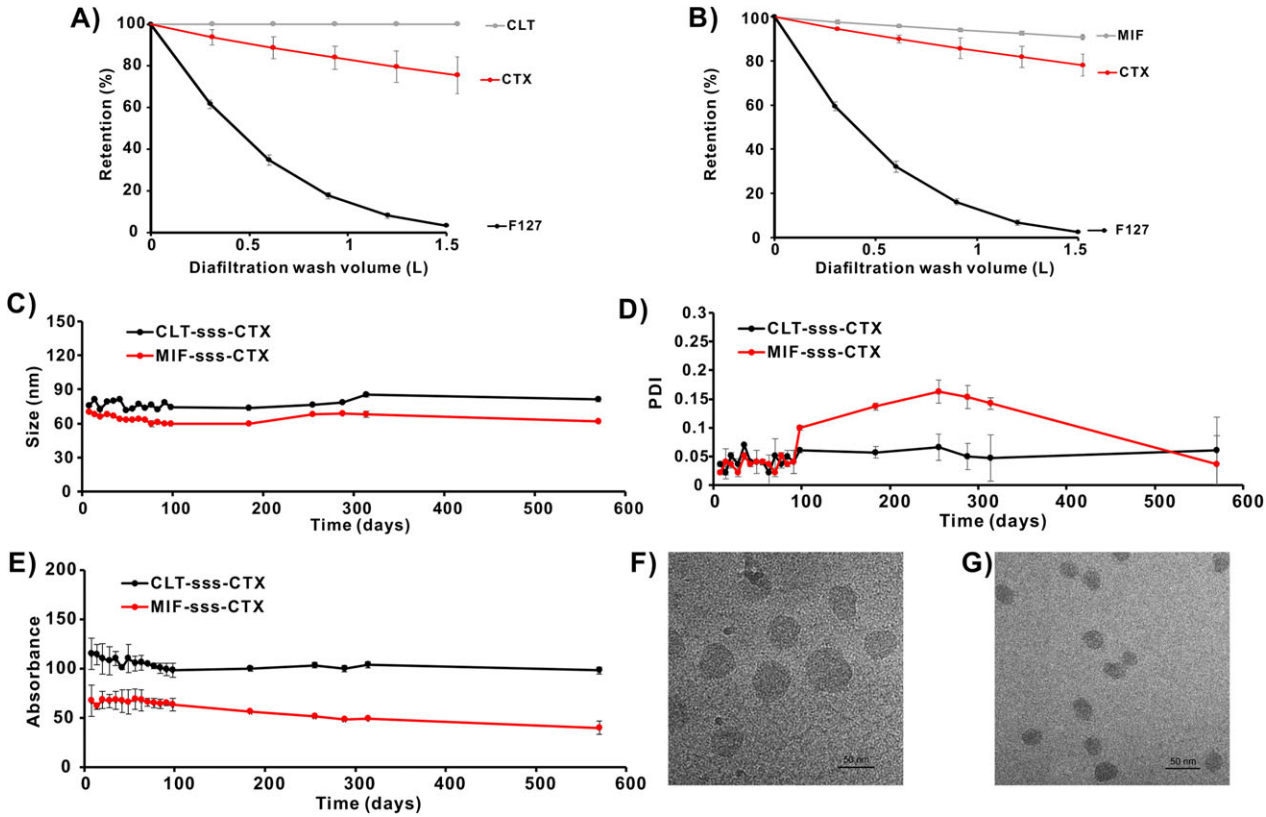

Figure 5. Scale up of sss-CTX. Drug, co-loader and F127 retention with A) 20% CLT or B) MIF co-loading in the large-scale washing process (at the 1.2 g CTX scale). C) Size for large-scale synthesized nanoparticle is stable over time. D) PDI for large-scale synthesized nanoparticle is stable over time. E) Absorbance after filtration for large-scale synthesized nanoparticle is stable over time. Stability data shows mean ± SD for 3 separate batches until day 100, then triplicate measurements for the same batch from day 100 to day 600. Cryo-EM image of F) CLT-sss-CTX and G) MIF-sss-CTX. A 50 nm scale bar is indicated.

Table 1. Composition of large-scale sss-CTX preparations.

	CLT-sss-CTX	MIF-sss-CTX
Cabazitaxel [mg mL^{-1}]	3	3
Co-loader [mg mL^{-1}]	1.82 ± 0.1 (CLT)	1.02 ± 0.1 (MIF)
F127 [mg mL^{-1}]	10.1 ± 2.6	10.7 ± 2.8
Drug to Surfactant mass ratio	1 : 3.4	1 : 3.6
Drug to Surfactant molar ratio	4.5 : 1	4.2 : 1

±Values show mean with SD for $n = 3$ preparations.

multiple dosing regimes were used since CTX was found to induce weight loss in mice at the heavier dosing. The average tumor volume and mice weight were monitored during the treatment period as **Figure 8** shows. At the dose of 30 mg kg^{-1} × 2 as Figure 8A shows, MIF-sss-CTX and CLT-sss-CTX delayed tumor growth and has statistical difference compared to a TWEEN-80 CTX group. From mice weight measurement, 30 mg kg^{-1} × 2 dose induced more body weight loss, compared to the lower total drug dosing regimes. At a dose of 15 mg kg^{-1} × 3 injections, CLT-sss-CTX had again a statistical improvement in tumor volume compared to a TWEEN-80 formulation, whereas MIF-sss-CTX did not (Figure 8C). At a dose of 8 mg kg^{-1} × 3, the CTX formulation could not suppress the tumor growth effectively (Figure 8E). Therefore, sss-CTX appeared to be equivalent or only slightly more effective than the TWEEN-80 formulation at equivalent dosing. Any mechanism for enhanced efficacy is not clear, but it is also noted that the sss-CTX formulations also appeared to induce slightly greater weight loss than the TWEEN-80 formulation at the higher dosing used (Figure 8D).

2.8. Histology Analysis of Solid Tumor Treatment

Histology analysis was performed to evaluate the therapeutic effects of CLT-sss-CTX and MIF-sss-CTX nanoparticles on the 4T1 orthotopic solid tumors (**Figure 9**). Hematoxylin and esosin (H&E) staining of the CTX treatment group reveals tumor with more empty space, possibly suggesting a loss in cell membrane integrity. Compared to control group, the Ki67 signal of CTX treatment group has less signal density, showing a reduction in cell proliferation. TUNEL staining confirmed tumor cells underwent apoptosis following treatment.

2.9. Neutropenia

A limiting clinical side effect of CTX is neutropenia. The impact of sss-CTX on neutropenia was assessed in healthy BALB/c mice

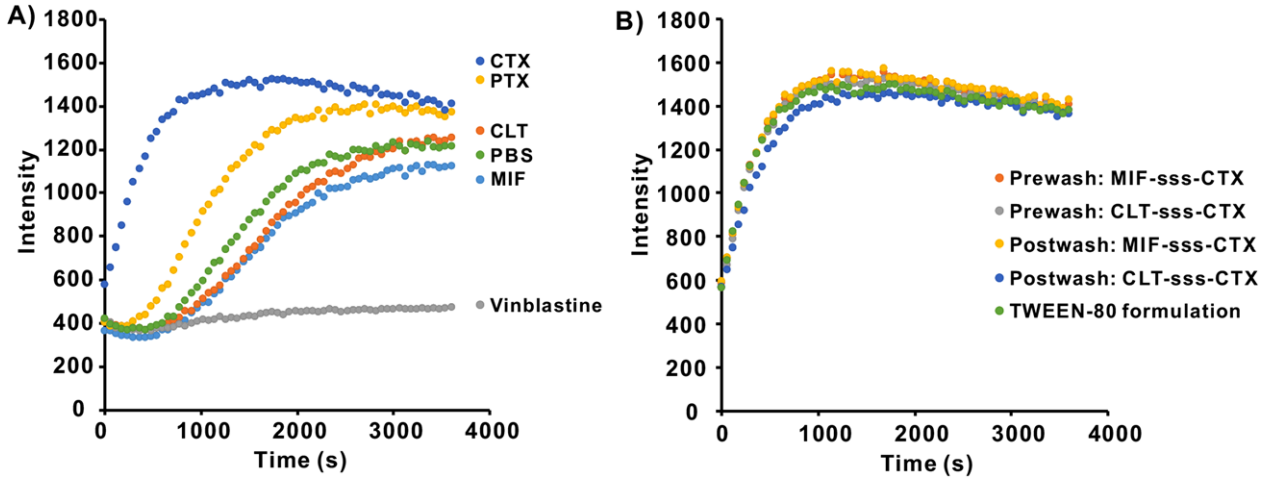

Figure 6. CTX accelerates tubulin polymerization, regardless of co-loaders or surfactant-stripping. A) Standard tubulin polymerization reaction rate as impacted by various drugs at 10 μM drug concentration. B) Standard tubulin polymerization reaction rate as impacted by various CTX formulations at 10 μM drug concentration. Results are shown from a single experiment.

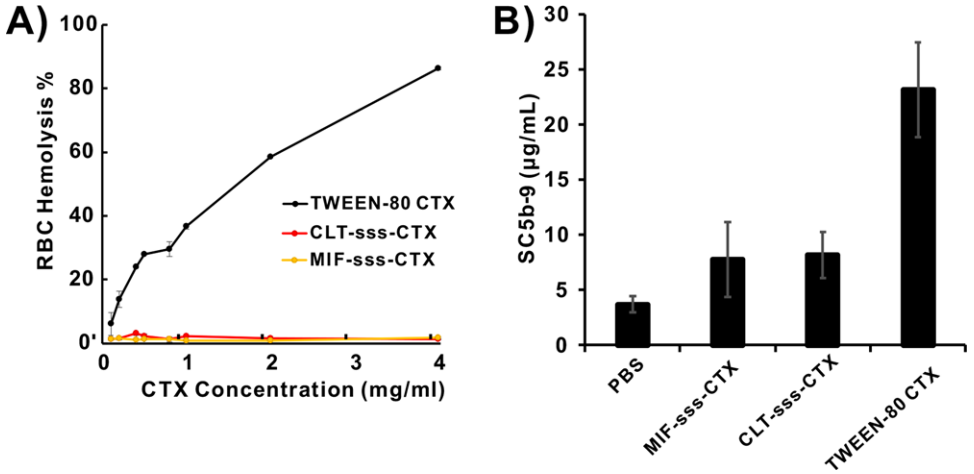

Figure 7. Blood interaction with sss-CTX. A) Hemolysis activity following CTX incubation with human red blood cells with different CTX formulations. B) Complement activation assay with various CTX formulations at 1 mg mL^{-1} in human plasma. Data shown mean +/− std. dev. for triplicate samples.

(**Figure 10**). With a single intravenous injection of CTX at a dose of 3, 10, or 20 mg kg^{-1}, the neutrophils in healthy mice dropped drastically after 3 days, compared to a control group. However, after 1-week recovery, the neutrophil count rebounded, apparently even higher than the pre-injection neutrophil count. There was no difference between the TWEEN-80 CTX group and the sss-CTX groups. Therefore, surfactant-stripping did not appear to inhibit or encourage neutropenia relative to the current clinical formulation. Comparing sss-CTX to the simpler TWEEN-80 formulation, similar levels of neutropenia were induced, there was no reduction in treatment-induced weight-loss at higher doses (Figure 8) and both behaved similarly in the tubulin polymerization assay (Figure 6B). The sss-CTX approach, while reducing the surfactant-content, did not reduce the toxicity of the formulation in these conditions, which is a desirable goal with new taxane formulations. Alternative approaches, such as chemically-modified prodrug carrier formulations may be promising in this regard.[32–35]

2.10. Serum Pharmacokinetics

The serum circulation of sss-CTX was assessed using an LC-MS method that used a deuterated CTX internal reference with nanogram sensitivity. Mice were intravenously administrated CTX formulations at the dose of 10 mg kg^{-1} and the serum was thereafter assessed for CTX levels (**Figure 11**). Based on non-compartmental analysis, the CTX half-life of the TWEEN-80 formulation was 9.35 h, which was similar, but slightly longer than MIF-sss-CTX (7.19 h) and CLT-sss-CTX (7.75 h). The TWEEN-80 formulation produced similar blood exposure as MIF-sss-CTX, exhibiting an AUC of 6864 ng mL^{-1} × h and 6285 ng mL^{-1} × h,

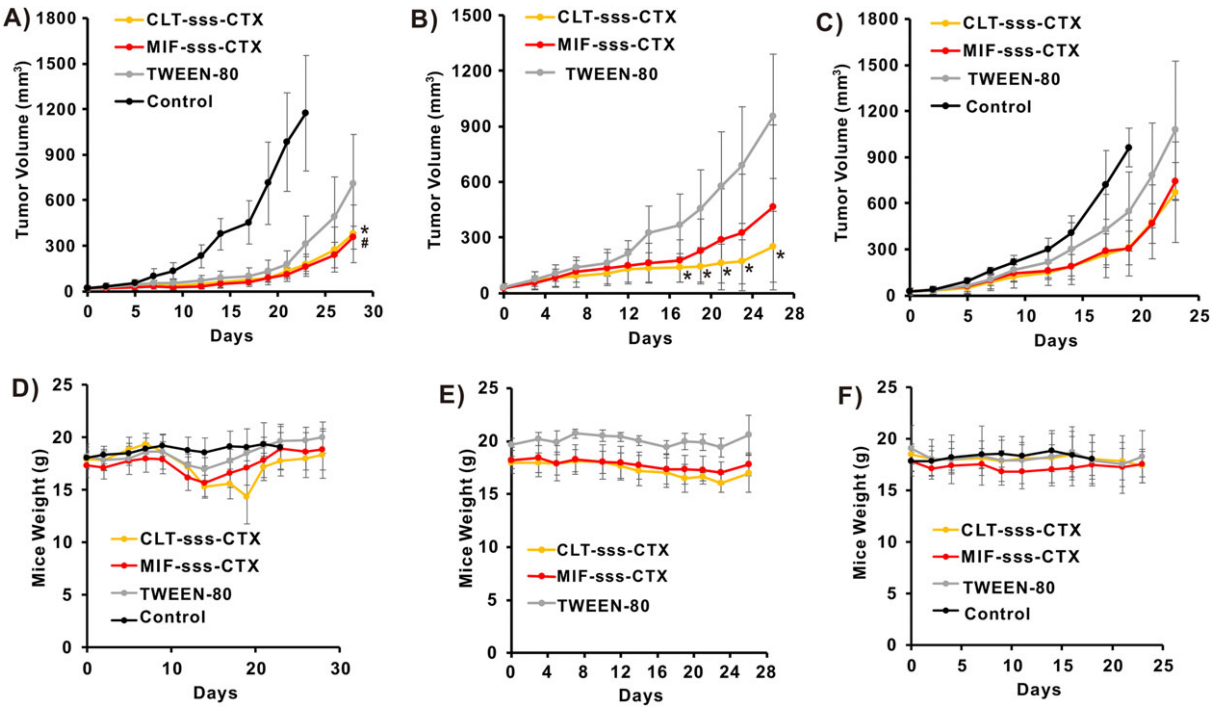

Figure 8. A antitumor efficacy of CTX formulations in mice bearing orthotopic 4T1 mammary tumors. Tumor volume and mice weight curves of: A,D) 2 injections of 30 mg kg^{-1} CTX days 1 and 5 (CLT-sss-CTX $n = 7$, MIF-sss-CTX $n = 6$, TWEEN-80 $n = 5$, control $n = 7$); B,E) 3 injections of 15 mg kg^{-1} CTX on days 1, 3, and 5 ($n = 5$); C,F) 3 injections of 8 mg kg^{-1} on days 1, 3, and 5 ($n = 6$). For tumor growth curves, * shows where CLT-sss-CTX group had significant difference and # shows MIF-sss-CTX group had significant difference, compared to the TWEEN-80 group ($p < 0.05$, one-way ANOVA with Tukey's posthoc pairwise comparison). Tumors in the sss-CTX groups were not significantly different from TWEEN-80 group in Fig. 8C.

respectively. CLT-sss-CTX had a longer circulation clearance with an AUC of 13 703 ng mL^{-1} × h. This may potentially be due to a role of CLT as a potent CYP3A inhibitor, a liver enzyme that degrades CTX and helps it clear out of the body.[36] That possibility raises an interesting question, which is whether the co-loaders themselves may have an impact on therapeutic outcomes. This was not examined in detail in this work, but the anti-tumor results show that any co-loader impact on anti-tumor efficacy was modest. This is not always the case, and one of the co-loaders examined, itraconazole, was shown to enhance efficacy when co-formulated with PTX and stabilize micelles.[37,38] In general, benign and inert co-loaders that are generally recognized as safe (which CLT and MIF are not) would avoid safety concerns and simplify data interpretation.

3. Conclusion

We carried out a screen of hydrophobic cargos to assess which, if any, stabilized surfactant-stripped CTX micelles. We identified MIF and CLT as particularly effective for providing long-term storage stability to CTX in aqueous formulations. These two drugs were also effective in stabilizing other taxane formulations. With the exceptions of higher drug-to-surfactant-ratio, and improved aqueous storage stability, the behavior of stabilized, surfactant-stripped CTX was generally similar to the current TWEEN-80 formulation. Taken together, these data show that the use of co-loaders can stabilize aqueous taxane formulations with high drug-to-surfactant ratios without detrimental effect on anti-cancer performance compared to conventional surfactant formulations.

4. Experimental Section

Materials: CTX was obtained from Carbosynth (# FC19621), and DTX and (PTX) were obtained from Avachem (# 1512 and # 1364, respectively). Deuterated CTX was obtained as a 1 mg reference standard from Toronto Research Chemicals (# C046502-1MG) The following surfactants, co-loaders, additional chemicals and solvents were used: F127 (Sigma # P2443), polysorbate 80 (VWR # EM-9490), Cremophor EL (Sigma # C5135), abamectin (Alfa Aesar # J60039), amiodarone (Alfa Aesar # J60456), azithromycin (Zithromax, TCI #A2076), β-carotene (TCI # C0560), budesonide (Fluka # P500178), carbamazepine (Sigma #C4024), chlorpromazine (TCI #C2481), cholecalciferol (Sigma #C59756), clofazimine (Sigma # C8895), CLT (Alfa Aesar # J63895), chloroquine (Sigma #C6628), coenzyme Q-10 (Alfa Aesar #J65137), cyclizine (Sigma # S361267), cyclosporin A (LC Labs # C6000), doramectin (Carbosynth # FD225991301), econazole (spectazole, VWR # AAJ63173-06), epothilone B (LC Labs # E5500), ergocalciferol (Sigma # E5750), erythromycin (Sigma # E5389), etoposide (VWR # 102610-708), fenofibrate (Sigma #F6020), finasteride (Enzo #L23536A), fluconazole (TCI #F0677), fulvestrant (Sigma # I4409), haloperidol (Sigma # H1512), haloperidol decanoate (halomonth; Sigma # H0100100), itraconazole (TCI #I0732), ivermectin (VWR # AAJ62777), ketoconazole (Alfa Aesar # J63367), labetalol (Sigma # L1011), meloxicam (TCI # M1959), miconazole (Alfa Aesar # J60459), nimodipine (TCI # N0896), novobiocin (Sigma # N1628), pregnenolone (antofin, TCI # P0477), progesterone (Acros # 225650050), sibutramine (meridia; Enzo #03271312), simvastatin (Ark Pharm # AK48916),

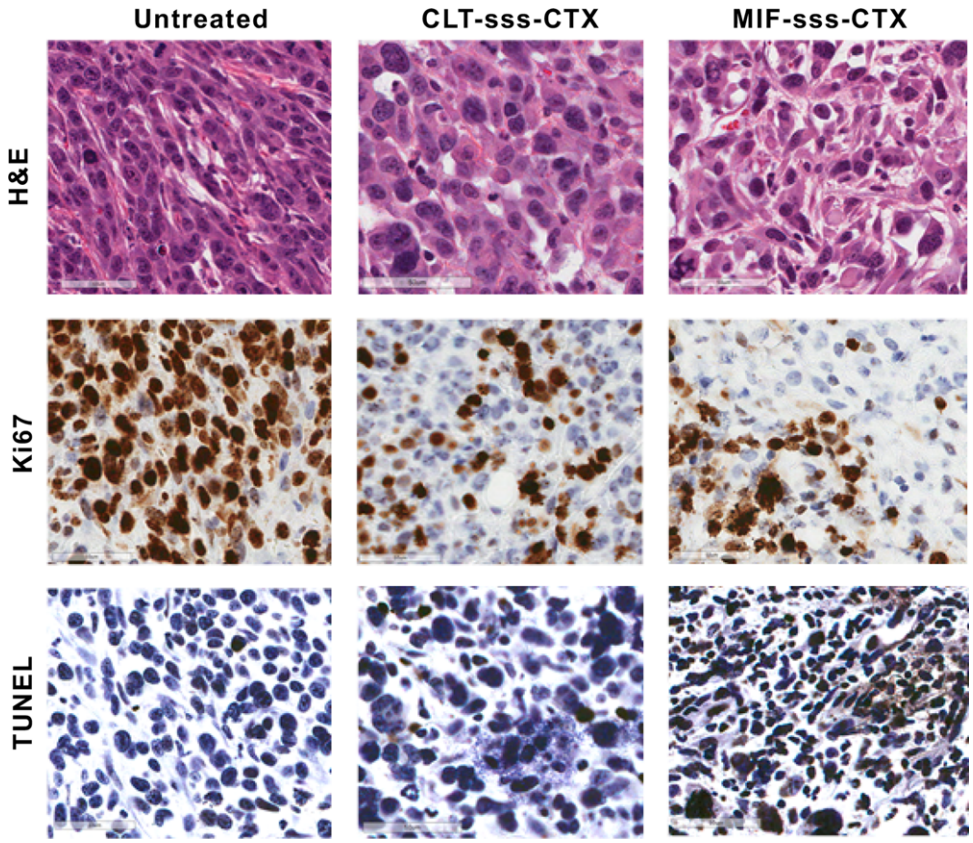

Figure 9. H&E, KI67, and TUNEL staining of tumor tissue harvested from mice bearing 4T1 orthotopic tumors treated with either CLT sss-CTX or MIF sss-CTX. Tumor tissue was harvested 72 h post injection. Scale bar indicates 50 μm.

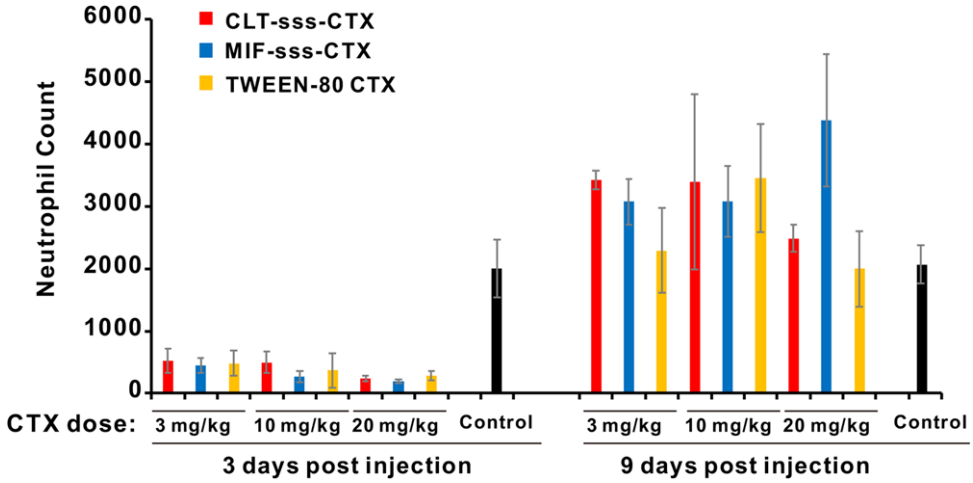

Figure 10. Neutropenia induction following a single CTX dose. Neutrophils in blood of BALB/c mice were counted following a single intravenous CTX injection at the indicated dose, formulation and time following injection ($n = 6$ mice per group).

MIF (TCI # M1732), mycophenolate mofetil (cellcept; Sigma # SML0284), piroxicam (Sigma # P5654), rifampicin (Sigma # R8883), reserpine (Sigma # R0875), selamectin (BOC # B15W019919), tacrolimus (Carbosynth # AT232931501), tamoxifen (MP # 7198K), testosterone undecanoate (Finetech # FT0635916), triamcinolone (Sigma #T6501), tolnaftate (Alfa Aesar # J61834), tioconazole (Alfa Aesar # J60459), tocopherol polythylene glycol (1000 succinate) (Sigma #57668), Vitamin C (Sigma # 57668), cobalt nitrate hexahydrate(Alfa Aesar #36418), ammonium thiocyanate (Alfa Aesar #A10632), ethyl acetate, acetone and methylene chloride (Fisher), and ethanol (Decon).

Taxane Aggregation in F127 Micelles: Various weight of taxanes were dissolved in 0.2 mL DCM, and then slowly dropped to a 1 mL 10% F127 solution with stirring for 5 h. The resulting clear solution was then centrifuged at 5000 × *g* for 5 min, the supernatant was discarded, the

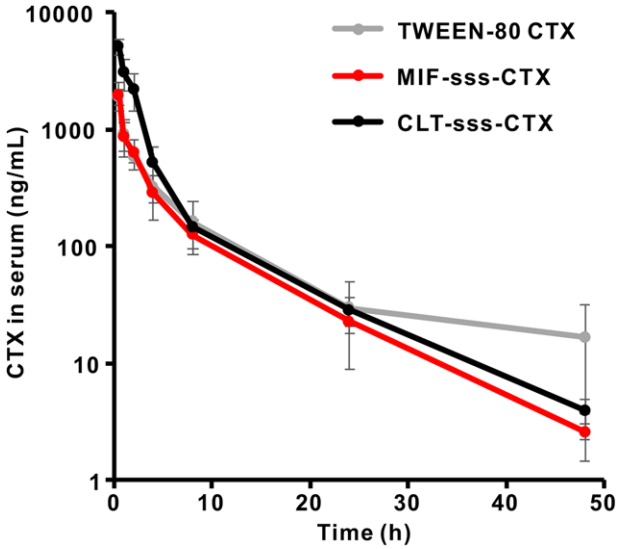

Figure 11. Serum pharmacokinetic profile of CTX formulations. Mean serum pharmacokinetics profile of CTX in BALB/c mice after a single intravenous dose of 10 mg kg^{-1} ($n = 4$).

pellet was washed by PBS twice and dissolved in 1 mL ethanol. The sample absorbance was measured by Lambda XLS spectrophotometer (PerkinElmer) using quartz cuvettes with 1 cm path length for regular absorbance measurement at 230 nm. To assess the kinetics of CTX precipitation, 4 mg CTX was dissolved in 0.2 mL DCM, and then dropped to a 1 mL 10% F127 solution with stirring for 5 h. The resulting clear solution was diluted to 1 in 15 in PBS solution and agitated in a Bioshaker XP at 500 rpm in 2 mL microcentrifuge tubes at room temperature. At various time points, the sample was centrifuged at 5000 × *g* for 5 min, the pellet was washed by PBS twice and dissolved in 1 mL ethanol. The absorbance was measured at 230 nm to assess precipitation.

Physical Characterization: 4 mg CTX was dissolved in 0.2 mL DCM, and then dropped to a 1 mL 10% F127 and stirred until clear. After several days, the precipitation was obtained by centrifugation and washed twice by water. The resulting precipitation was freeze-dried, the resulting white solid was coated with gold and performed by SEM. The co-loaded sss-CTX were obtained from the stability test after 600 days storage with the preparation steps. X-ray diffraction was carried out on a Rigaku Ultima IV with operating conditions 40 kV, 44 mA, and 1.76 kW. The source of the diffractometer used here was a Cu K α radiation at a 1.54 Å wavelength with a monochromator filter. The mode was analyzed in $\theta/2\theta$ mode at room temperature. The 2θ scan data were collected with a 0.030 interval, and a speed of 0.5° min^{-1}. The technique used for measuring intensities was the focusing beam method.

Preliminary Co-Loader Screen: 4 mg CTX and 1 mg co-loader was dissolved in 0.2 mL DCM, and then dropped to a 1 mL 10% F127 and was stirred for 5 h. The resulting solution was diluted to 1 in 15 in PBS solution and shanked by Bioshaker XP at 500 rpm in room temperature. After 2 days, the sample was centrifuged at 5000 × *g* for 5 min, the supernatant was discarded, the pellet was washed three times by using PBS solution and then dissolved in 1 mL ethanol and the absorbance was measured by Lambda XLS spectrophotometer (PerkinElmer) at 230 nm.

Co-Loading Inhibits Aggregation in Other Cabazitaxel Formulation: To prepare a Taxol-like formulation, 12 mg PTX or 12 mg PTX plus 3 mg co-loader were dissolved in 1 mL ethanol and then mixed with 1 mL Cremphor EL solution in certain range concentration. To measure the PTX concentration, 10 µL of the supernatant solution was dissolved in 990 µL of ethanol and absorption at 230 nm was measured. In the albumin-PTX study, 100 mg bovine serum albumin (BSA) was dissolved in 10 mL Tris buffer (5 mM) in 37 °C while stirring, and added 900 µL β-ME dropwise and stirred. The BSA solution was dispersed in 100 of ultrapure water while stirring at 37 °C, then added 350 µL β-ME. 9 mg PTX or 9 mg PTX plus 2.25 mg co-loader were dissolved in 9 mL ethanol, and was dropped to the stirring solution at 37 °C. At 0 h and 48 h, the supernatant absorbance was measured at 230 nm.

Further Screening Co-Loaders with Surfactant-Stripping: 4 mg CTX and 1 mg co-loader was dissolved in 0.2 mL DCM, and then was added dropwise to 1 mL 10% F127, and stirred for 5 h. The resulting solution was added to conical filtration devices (100 000 Da molecular weight cutoff; fisher # UCF9-100-24) and subjected to centrifugal filtration at 3000 × *g*, 4 °C. When 500 µL of concentrate was left, cold PBS was added back and the washing procedure was repeated three times. Before washing and post washing, 10 µL of the solutions were added into 990 µL ethanol, and the absorbance was measured by Lambda XLS spectrophotometer (PerkinElmer) at 230 nm. To screen sss-CTX storage stability, the washed co-loaded solution was recalibrated to 500 µL, incubated in room temperature or 4 °C. Each week, the samples were vortexed until the samples were well mixed and then 20 µL of sample mixed with 1 mL water was taken, and centrifuged at 3000 × *g*. The supernatant was discarded and the pellet was washed two times with PBS. Then the pellet was dissolved in 1 mL ethanol and the absorbance was measured at 230 nm.

Large-Scale sss-CTX Synthesis: 300 mg CTX and 75 mg co-loader (MIF; or CLT) were dissolved in 20 mL DCM, and then added dropwise to 100 mL 10% F127 solution, and was stirred until the organic solvent evaporated (typically 5 h). The resulting clear solution was diluted with PBS to 500 mL and subjected to diafiltration at 4 °C (Sartorius Vivaflow # 1501008VS) to remove excessive F127 until 100 mL concentrate was left. Cold PBS solution was added back and the wash process was repeated 5 times, with each wash the filtrates were sampled 2 mL for drug and F127 quantification. The large-scale batch was further concentrated by centrifugal filtration and filtered through a 0.45 µm syringe filter.

Drug and F127 Quantification: To quantify CTX, 10 µL of the sample was mixed with 190 µL DMSO and centrifuged at 5000 × *g* for 1 min, the supernatant was injected for HPLC analysis (Water Alliance 2790 instrument). The elution gradient was from 30 to 80% acetonitrile in 0.1% trifluoroacetic acid in water at room temperature. The measurement wavelengths were 302 nm (for MIF), 230 nm (for CTX), and 237 nm (CLT). To quantify F127, 100 µL of cobalt thiocyanate solution, 40 µL samples in the concentration range of 0–7.5 wt%, 200 µL ethyl acetate and 80 µL ethanol were mixed and vortexed for 10 s. The cobalt thiocyanate was prepared by dissolving 0.3 g cobalt nitrate hexahydrate and 1.2 g ammonium thiocyanate in 3 mL water. After mixing, the sample was vortexed for 10 s and centrifuged at 10 000 × *g* for 3 min. The blue supernatant was removed and the blue pellet was washed using ethyl acetate several times until the washed supernatant had no color. The pellet was dissolved in 1 mL acetone and the absorbance at 625 nm was measured by a Lambda XLS spectrophotometer (PerkinElmer).

CTX Stability: sss-CTX nanoparticle stability was monitored both for size and drug retention. The size was measured with DLS using a NanoBrook 90 plus PALS instrument (Brookhaven Instruments). For drug retention measurement, 15 µL of sample supernatant was added to 1485 µL of PBS and mixed, passed through 200 nm nylon filter and 1 mL of the filtered solution was used to measure the absorbance at 230 nm.

Cryo-Electron Microscopy: Holey carbon grids (c-flat CF-2/2-2C-T) previously washed with chloroform were glow-discharged at 5 mA for 15 s immediately before sample application. A volume of 3.6 µL of each sample was deposited in the EM grid. The concentration of the applied samples was 2 mg mL^{-1}. Vitrification was performed in a Vitrobot Mark IV (ThermoFisher) by blotting the grids once for 3 s with blot force +1 before they were plunged into liquid ethane. Temperature and relative humidity during the vitrification process were maintained at 25 °C and 100%, respectively. The grid was loaded into the Tecnai F20 electron microscope operated at 200 kV using a Gatan 626 single tilt cryo-holder. Images were collected in a Gatan Ultrascan 4000 4k × 4k CCD Camera System Model 895 at a nominal magnification 80 000×, which produced images with a calibrated pixel size of 1.41 Å per pixel. Images were collected with a total dose of 50 e^{-} $Å^{-2}$ using a defocus ranging from −2.7 to −3.5 µm. Images were cropped and prepared for figures using Adobe Photoshop program.

In Vitro Hemolysis: For the hemolysis study, fresh human erythrocytes were collected in citrate from healthy human volunteers. The erythrocyte suspension was obtained by centrifugation at 240 × *g* for 13 min with brake setting 0. The erythrocyte suspension was washed by PBS solution five times at 1200 × *g* for 5 min with brake setting 2. PBS solution was added to form an erythrocyte suspension in the original whole blood volume and mixed. 15 µL of erythrocyte was mixed with 5 µL of CTX formulations at different concentrations and was incubated at 37 °C for 1 h. 1 mL PBS was added and centrifuged at 3000 × *g* for 5 min. PBS and dilute Triton X-100 solution were used as negative (0% lysis) and positive controls (100% lysis), respectively. The absorbance of the supernatant was measured at 540 nm.

Animal Studies: All animal studies were carried out in compliance with University at Buffalo IACUC protocols. For tumor studies, 4T1 cells were injected orthotopically into the mammary fat pad of female BALB/c mice and the treatment began when the tumor volumes reached 100 mm^3. A Jevtana-like TWEEN-80 formulation was prepared by dissolving 40 mg CTX in 1 mL TWEEN-80, followed by vortexing until the drug was completely dissolved. Before injection, 3 mL of 13% (w/w) ethanol aqueous solution was added to prepare the injection solution. CTX formulations were administered intravenously via tail-vein as indicated. Tumor size and mouse weight were monitored three times per week. Mice were sacrificed when the tumor size reached 10 times the original volume. For neutrophils study, three groups of female BALB/c mice were intravenously injected with CLT-sss-CTX, MIF-sss-CTX and the TWEEN-80 formulation. After 3 days, 200 µL of blood was taken retro-orbitally with the anticoagulant EDTA, and the blood was subjected to neutrophils quantification experiment within 30 min in room temperature. 10 µL mouse blood incubated with 1:1000 LDS, 1:100 FITC-CD11b, 1:100 PE-GR1(1A8-Ly6g) at 37 °C for 10 min. 200 µL lysis buffer was added and incubated on ice for 10 min, and flow cytometry was conducted.

Histology Analysis: 5×10^4 4T1 cells were injected in BALB/c mice to induce orthotopic tumors. 30 mg kg^{-1} (200 µL) of CLT-sss-CTX or MIF-sss-CTX solution was injected intravenously via tail vein in tumor induced BALB/c mice. Control mice bearing orthotopic tumor remained untreated. Mice were sacrificed 72 h after drug was injected and tumor tissue was harvested. Tumor tissue was immediately immersed in 10% formalin and was stored overnight. Tissues were then transferred to 70% ethanol and were further processed for H&E, Ki67, and TUNEL immunohistochemistry staining as previously described.[39] Stained tumor tissue slides were imaged using Aperio Scanscope and resized using Imagescope software.

Tubulin Polymerization: The kinetics of tubulin polymerization were determined by tubulin polymerization assay kit (BK006P, Cytoskeleton, Dever, Co., USA). The purified porcine brain tubulin was diluted with tubulin buffer to 3 mg mL^{-1} and frozen in −80 °C until use. To measure the tubulin polymerization rate, the tubulin solution was mixed with 10% glycerol, 1 mM GTP and 10 µM drug formulations. The mixture was preheated to 37 °C and quickly transferred to a 96 plate reader to read absorbance every minute for 30 min at 340 nm at 37 °C.

Pharmacokinetics: CTX concentrations in serum were evaluated in twelve BALB/c mice after intravenous administration of the CTX formulations at a dose of 10 mg kg^{-1}. Blood samples (50 µL) were collected from the ophthalmic vein at 0.5, 1, 2, 4, 8, 24, and 48 h after intravenous-administrated CTX treatment. The blood samples were centrifuged at 2000 rpm for 10 min, the serum was collected and stored at −20 °C until HPLC analysis. To process the serum sample, 300 µL *tert*-butyl methyl ether was added, and the sample was vortexed and sonicated for 30 min until it was mixed. Then the sample was centrifuged at 10 000 rpm 3 min and the *tert*-butyl methyl ether supernatant was collected. *Tert*-butyl methyl ether extraction was repeated and the collected *tert*-butyl methyl ether was dried by nitrogen purging until dry. 150 µL 50% acetonitrile/water was added to each sample and vortexed until well mixed. The sample was transferred to HLPC vials with inserts for analysis by LC/MS. Analysis by LC/MS was performed using a Sciex API 3000 triple quadrupole mass spectrometer equipped with a Turboionspray source and a Shimadzu Prominence HPLC system. The HPLC system included 2 LC20AD pumps, an online DGU-20A_{5R}degasser, a CTO-20AC column oven and a SIL-20AC autosampler. The analytical column was a Waters 2.1. × 100 mm XSelect CSH C18 column (particle size 3.5 µm). The injection volume was 10 µL, and the needle wash was 50/50 and 70/30 Acetonitrile /water. The LC flow rate was 200 µL min^{-1}. The mobile phases consisted of (A) 5/95 Acetonitrile/water +0.1% formic acid, and (B) 95/5 Acetonitrile/water +0.1% formic acid. The starting mobile phase was 60% B and was increased to 95% B over 5 min, it was held at 95% for 3 min before re-equilibrating for 5 min. MRM (Multiple reaction monitoring) conditions for the CTX including *m/z* of MRM pairs, collision energy, and orifice potential, were optimized by flow injection analysis. The MRM transitions for CTX and the deuterated internal standard (d6-cabazitaxel) were 836.7/555.5 and 842.5/561.4, respectively. The LC/MS, the dwell time of each MRM transition was 300 ms, and the pause time for scan parameter changes was 5 ms. The ion spray voltage, declustering potential, collision energy, and source temperature were 5500 V, 22, 15, and 400 °C, respectively. The CTX quantification limits were 2.5 ng mL^{-1}. Pharmacokinetic parameters were extracted with PKSolver in Excel software.

Statistical Analysis: Statistical analysis was performed with GraphPad Prism 8.0.

Supporting Information

Supporting Information is available from the Wiley Online Library or from the author.

Acknowledgements

The authors acknowledge the support of Jumin Geng for animal studies, Haoyuan Huang for assistance with SEM, and Xuedan He for assistance with complement measurement. The authors thank Kelly Sears, Mike Strauss, Kaustuv Basu, and other staff members of the Facility for Electron Microscopy Research (FEMR) at McGill University for help in microscope operation and data collection. FEMR is supported by the Canadian Foundation for Innovation, Quebec government and McGill University. This work was supported by the National Institutes of Health (DP5OD017898 and R01EB017270) and the National Science Foundation (1555220).

Conflict of Interest

The authors declare no conflict of interest.

Keywords

cabazitaxel, chemotherapy, drug delivery, micelles

Received: August 13, 2019
Revised: October 31, 2019
Published online:

[1] M. A. Jordan, L. Wilson, *Nat. Rev. Cancer* **2004**, *4*, 253.
[2] R. Yusuf, Z. Duan, D. Lamendola, R. Penson, M. Seiden, *Curr. Cancer Drug Targets* **2003**, *3*, 1.
[3] P. Vrignaud, D. Sémiond, P. Lejeune, H. Bouchard, L. Calvet, C. Combeau, J.-F. Riou, A. Commerçon, F. Lavelle, M.-C. Bissery, *Clin. Cancer Res.* **2013**, *19*, 2973.
[4] J. S. De Bono, S. Oudard, M. Ozguroglu, S. Hansen, J.-P. Machiels, I. Kocak, G. Gravis, I. Bodrogi, M. J. Mackenzie, L. Shen, *Lancet* **2010**, *376*, 1147.
[5] M. D. Galsky, A. Dritselis, P. Kirkpatrick, W. K. Oh, *Nat. Rev. Drug Discovery* **2010**, *9*, 677.
[6] B. Sun, R. M. Straubinger, J. F. Lovell, *Nano Res.* **2018**,*11*, 5193.

[7] G. Zhou, X. Jin, P. Zhu, J. U. Yao, Y. Zhang, L. Teng, R. J. Lee, X. Zhang, W. Hong, *Anticancer Res*. **2016**, *36*, 1649.
[8] N. Qu, R. J. Lee, Y. Sun, G. Cai, J. Wang, M. Wang, J. Lu, Q. Meng, L. Teng, D. Wang, L. Teng, *Int. J. Nanomed*. **2016**, *11*, 3451.
[9] Y. Sun, Y. Zhao, S. Teng, F. Hao, H. Zhang, F. Meng, X. Zhao, X. Zheng, Y. Bi, Y. Yao, R. J. Lee, L. Teng, *Int. J. Nanomed*. **2018**, *14*, 135.
[10] N. Qu, Y. Sun, J. Xie, L. Teng, *Anti-Cancer Agents Med. Chem*. **2017**, *17*, 294.
[11] N. Kommineni, S. Mahira, A. J. Domb, W. Khan, *Pharmaceutics* **2019**, *11*, 141.
[12] X. Yin, L. Luo, W. Li, J. Yang, C. Zhu, M. Jiang, B. qin, X. Yuan, H. Yin, Y. Lu, Y. Du, D. Chen, J. You, *Asian J. Pharm. Sci*. **2018**, *14*, 658.
[13] N. Kommineni, R. Saka, U. Bulbake, W. Khan, *Chem. Phys. Lipids* **2018**, *224*, 104707.
[14] A. Ahmad, S. Sheikh, M. Paithankar, G. Deshpande, K. C. Lakshmaiah, T. M. Maksud, A. Khatri, M. K, P. Kale, R. Patel, H. Barkate, I. Ahmad, *J. Clin. Oncol*. **2016**, *34*, e14019.
[15] X. Han, F. Gong, J. Sun, Y. Li, X. Liu, D. Chen, J. Liu, Y. Shen, *J. Nano. Res*. **2018**, *20*, 42.
[16] O. Aydin, I. Youssef, Y. Yuksel Durmaz, G. Tiruchinapally, M. E. H. ElSayed, *Mol. Pharmaceutics* **2016**, *13*, 1413.
[17] A. S. Gdowski, A. Ranjan, M. R. Sarker, J. K. Vishwanatha, *Nanomedicine*. **2017**, *12*, 2083.
[18] J. Wan, Y. Qiao, X. Chen, J. Wu, L. Zhou, J. Zhang, S. Fang, H. Wang, *Adv. Funct. Mater*. **2018**, *28*, 1804229.
[19] J. Bteich, M. J. Ernsting, M. Mohammed, T. Kiyota, T. D. McKee, M. Trikha, H. B. Lowman, K. K. Sokoll, *Bioconjugate Chem*. **2018**, *29*, 2009.
[20] Z. Lu, T. Li, L. Ren, L. Zhou, J. Wan, J. Wu, Y. Qiao, H. Xie, S. Zheng, H. Wang, *J. Biomed. Nanotechnol*. **2018**, *14*, 1853.
[21] F. Bensaid, O. Thillaye du Boullay, A. Amgoune, C. Pradel, L. Harivardhan Reddy, E. Didier, S. Sablé, G. Louit, D. Bazile, D. Bourissou, *Biomacromolecules* **2013**, *14*, 1189.
[22] W. N. Waugh, L. A. Trissel, V. J. Stella, *Am. J. Health-Syst. Pharm*. **1991**, *48*, 1520.
[23] A. Sparreboom, L. van Zuylen, E. Brouwer, W. J. Loos, P. de Bruijn, H. Gelderblom, M. Pillay, K. Nooter, G. Stoter, J. Verweij, *Clin. Pharm. Implications* **1999**, *59*, 1454.
[24] V. R. N. Panday, M. T. Huizing, W. W. Ten Bokkel Huinink, J. B. Vermorken, J. H. Beijnen, *Clin Microbiol. Infect*. **1997**, *14*, 418.
[25] Y. Zhang, M. Jeon, L. J. Rich, H. Hong, J. Geng, Y. Zhang, S. Shi, T. E. Barnhart, P. Alexandridis, J. D. Huizinga, M. Seshadri, W. Cai, C. Kim, J. F. Lovell, *Nat. Nanotechnol*. **2014**, *9*, 631.
[26] Y. Zhang, W. Song, J. Geng, U. Chitgupi, H. Unsal, J. Federizon, J. Rzayev, D. K. Sukumaran, P. Alexandridis, J. F. Lovell, *Nat. Commun*. **2016**, *7*, 11649.
[27] P. Vrignaud, D. Semiond, V. Benning, E. Beys, H. Bouchard, S. Gupta, *Drug Des., Dev.Ther*. **2014**, *8*, 1851.
[28] M. Bohorquez, C. Koch, T. Trygstad, N. Pandit, *J. Colloid Interface Sci*. **1999**, *216*, 34.
[29] M. Green, G. Manikhas, S. Orlov, B. Afanasyev, A. Makhson, P. Bhar, M. Hawkins, *Ann. Oncol*. **2006**, *17*, 1263.
[30] W. J. Gradishar, D. Krasnojon, S. Cheporov, A. N. Makhson, G. M. Manikhas, A. Clawson, P. Bhar, *J. Clin. Oncol*. **2009**, *27*, 3611.
[31] Z. Weiszhár, J. Czúcz, C. Révész, L. Rosivall, J. Szebeni, Z. Rozsnyay, *Eur. J. Pharm. Sci*. **2012**, *45*, 492.
[32] H. Wang, L. Zhou, K. Xie, J. Wu, P. Song, H. Xie, L. Zhou, J. Liu, X. Xu, Y. Shen, S. Zheng, *Theranostics* **2018**, *8*, 3949.
[33] H. Wang, Z. Lu, L. Wang, T. Guo, J. Wu, J. Wan, L. Zhou, H. Li, Z. Li, D. Jiang, P. Song, H. Xie, L. Zhou, X. Xu, S. Zheng, *Cancer Res*. **2017**, *77*, 6963.
[34] B. Yang, K. Wang, D. Zhang, B. Sun, B. Ji, L. Wei, Z. Li, M. Wang, X. Zhang, H. Zhang, Q. Kan, C. Luo, Y. Wang, Z. He, J. Sun, *Biomater. Sci*. **2018**, *6*, 2965.
[35] P. Xue, D. Liu, J. Wang, N. Zhang, J. Zhou, L. Li, W. Guo, M. Sun, X. Han, Y. Wang, *Bioconjugate Chem*. **2016**, *27*, 1360.
[36] M. A. Gibbs, K. L. Kunze, W. N. Howald, K. E. Thummel, *Drug Metab. Dispos*. **1999**, *27*, 596.
[37] Z. Liu, L. Zhang, Z. Tian, C. Kong, C. Liu, H. Liu, F. Yuan, W. Kong, F. Qian, *Adv. Ther*, **2019**, *2*, 1900032.
[38] L. Zhang, Z. Liu, C. Kong, C. Liu, K. Yang, H. Chen, J. Huang, F. Qian, *Small* **2018**, *14*, 1802112.
[39] D. Luo, S. Goel, H. J. Liu, K. A. Carter, D. Jiang, J. Geng, C. J. Kutyreff, J. W. Engle, W. C. Huang, S. Shao, C. Fang, W. Cai, J. F. Lovell, *ACS Nano* **2017**, *11*, 12482.

